Egypt. J. Chem. **Vol. 66** No. 11 pp 15-24 (2023)

Egyptian Journal of Chemistry

http://ejchem.journals.ekb.eg/

Preparation, Characterization, and Rheological Behavior of O/W and W/O Non- Newtonian Emulsions using surface-modified Nano-Silica and Non-Ionic surfactant

Nabel A. Negm [1*], Mohamed Betiha, [2] Nermin Saleh [3]

[1] *Egyptian Petroleum Research Institute*
[2] *Petrolium Institute*
[3] *Egyptian petroleum research institute*

Abstract

This paper used rice husk residues to extract silica and turn it into a liquid sodium silicate product by sodium hydroxide. The silica structure was formed by utilizing a Pluronic 123 surfactant in acidic media to produce silica with a controlled and medium porosity. The silica surface was grafted with (3-aminopropyl)triethoxysilane compound and then reacted with 1,3-propane sultone to produce silica capped with sulfonate groups. HSO_3CF_3 was used to exchange the prepared material's counter ion for producing a highly acidic catalyst. The resulting catalyst was identified by various techniques, including HRTEM, XRD, BET, and FTIR. The results proved that the mesoporous materials had a surface area close to 769 m^2/g, and after making the modifications, the surface area reached 185 m^2/g. The catalyst was exploited in the preparation of 1-(2-hydroxyethoxy)-nonadecan-2-one compound, where it was obtained with a percentage close to 99.8% at a temperature of 140 °C and a catalytic amount of 8%. The resulting compound, 1-(2-hydroxyethoxy)-nonadecan-2-one, was mixed with sodium dodecyl sulfate to prepare oil in water emulsions. The results proved that the emulsion is stable for a period of up to 18 hours, and it depends on the percentage of oil in the emulsion. Oil's viscosity in water emulsion has greatly improved compared to water in oil emulsion stabilized with amide product attached to mesoporous silica. Several rheological models have been assigned to the description of the behavior of non-Newtonian emulsion.

Keywords: Functionalized mesoporous silica; non-Newtonian; rheological modes; emulsions

1. Introduction

The viscosity of extra heavy petroleum oil ranges from 103 mPa/s to 105 mPa/s at room temperature [1]. In contrast, the desired viscosity of the flow of crude oil through the pipeline is less than 200 MPa at 15 ° C [2]. Such extra heavy crude oils contain high levels of saturated paraffin and large quantities of resins and asphaltene, which reduces the possibility of their flow under normal conditions. In the petroleum industries, this problem represents a great specificity during production and transporting these raw materials to oil refineries. The processing of such crude is complicated and difficult, as it is difficult to transport the oil in the pipes due to the high viscosity or high pour point [3].

Among the heaviest components of crude oil is Asphaltene; Asphaltene consists of several interlocking chains of polycyclic aromatic groups intertwined by nitrogen or sulfur atoms, to which several aliphatic groups are attached to their ends [4]. This series includes trace amounts of metals with high oxidation states, such as vanadium. The asphaltene compound was considered amphiphilic molecules. It contains electron donor-acceptor and hydrogen bonding interaction between alkyl chain moieties or poly-condensed aromatic (lipophilic moieties) and

*Corresponding author e-mail: nabelnegm@hotmail.com
Receive Date: 14 November 2021, Revise Date: 22 November 2021, Accept Date: 18 September 2022
DOI: 10.21608/EJCHEM.2022.105977.4877

hetero-atom groups (hydrophilic moieties), allowing different interaction with hydrophilic and hydrophobic crude oil components, forming stable water in oil emulsion.

The emulsion usually consists of two immiscible liquid phases, one of which is dispersed as globules (dispersed phase) in the other liquid phase (continuous phase) [5]. There are three types of emulsions; water in oil (the dispersed phase is water globules which dispersed through the continuous phase, oil phase, and it is referred to as (W / O). Oil in water emulsion, in which oil globules are dispersed in the continuous phase (referred to as O / W). When W / O and O/W emulsions are dispersed throughout during another immiscible phase, they are called multiple emulsions. These emulsions can be found in many areas, either as a desirable or undesirable type, such as food processing, pharmaceutics, chemistry, and cosmetics [6-8]. O / W emulsion and W / O emulsions are often found in crude oil production or during pipeline transportation of crude oil.

Transporting heavy crude oil in pipelines depends on several approaches, including reducing friction between the crude oil and the inner surface of the transport pipelines, reducing the viscosity of crude oil, and improving the chemical composition of the oil, whether by removing asphalt, chemical additives, or the formation of emulsions. Drag-reducing material is used to reduce turbulence (drag force between crude oil and pipeline) in a pipe [9]; however, the drag-reducing material suffers from separation from crude oil when restored [10].

In this paper, silica was extracted from rice husk and treated with amino-organosilane moieties to produce a highly acidic catalyst for use in the preparation of 1-(2-hydroxyethoxy)-nonadecan-2-one compound. Silica modified with amine groups was also used in the reaction with stearic acid for producing amide compound to stabilize the water-in-oil emulsion. O/W and W/O emulsions will be prepared and stabilized with stearic acid-modified NH_2-Pr-SBA-15 and aminopropyl functionalized SBA-15**.** The emulsion rheological models Bingham plastic, Power, Casson model, and Herschel-Bulkley models were applied.

2. Experimental

2.1 Material

Non-ionic surfactant, Poly(ethylene glycol)-block-poly(propylene glycol)-block-poly(ethylene glycol, 5800 g/mol), stearic acid (≥98.5%), ethylene glycol (99.8%) hydrochloric acid (HCl, 37%), 1,3-propane sultone (98%), 3-aminopropyl triethoxysilane (APTES, 99%), sodium hydroxide (NaOH, ≥98%), sodium dodecyl sulfate (≥99.0%), 1,2-dichloroethane were purchased from Sigma–Aldrich. Rice husk was obtained from processing rice residues obtained from the governorate of Kafr El-Sheikh, Egypt.

2.2. Extraction of Silica from Rice Husk

The silica was extracted from rice husk with our previously published method **[11]**. The rice straw was ground after drying at 100 °C for 8 hours; then, the dried crushed husk was transferred to a flask pre-filled 920 ml distilled water and 35 grams of concentrated sulfuric acid. The mixture was stirred for 4 hours at 80 ° C. After lowering the temperature, 500 ml of water was added to reduce acidity, and the mixture was filtered. The product was washed several times until the pH of the filtrate reached 6.5, then dried at 120 °C for 4 hours before calcination. The product was calcined at 800 ° C under the airflow (50 ml/min). The soluble silica (Na_2SiO_3) was achieved by adding sodium hydroxide solution 11.4 g (189.747 mmol) to silica (75 mmol) with a molar ratio of ~0.4 at 70 °C for 36 h; sodium silicate was obtained as a colloidal solution.

2.3. Preparation of Tunable Porous Santa Barbara Amorphous (SBA-15)

SBA-15 nanomaterial was obtained using the hydrothermal approach in the presence of P123 as a structure-directing agent. 4 g of the surfactant (P123) was dissolved in 120 mL distilled water. Then the pH was adjusted with hydrochloric acid at 1.7. 10.4 grams of sodium silicate was added once to the previously prepared solution. The mixture was mechanically stirred at 40 °C for 4 hours; then, the mixture was transferred to an autoclave lined with a Teflon layer. The temperature was increased to 110 °C at a static condition for 48 hours. After self-cooling, the precipitate was filtered and washed with a mixture of water and ethanol to eliminate the surface agent and then dry at 100 °C for 8 hours. The result was roasted at 550 m for 10 hours under airflow

2.4. Preparation of aminopropyl Functionalized SBA-15 (

NH_2-Pr-SBA-15)

5 g of SBA-15 was added to a 2% (3-aminopropyl)triethoxysilane solution in toluene, and the mixture was heated to 115 °C for 12 hours. The precipitate was separated and washed several times with 1,2-dichloroethane to eliminate the remaining reactants.

2.5. Preparation of –SO_3H Functionalized NH_2-Pr-SBA-15 (SO_3-Pr-NH_3-Pr-SBA-15)

5 g of the resultant NH_2-Pr-SBA-15 was dispersed in 50 mL 1,2-dichloroethane, and 5 g of 1,3-propane sultone was added under stirring. Then, the mixture was refluxed at 80 °C for five h. The sample was separated from 1,2-dichloroethane by filtration and washed thoroughly with toluene and diethyl ether (30:70; v/v) to remove the unreacted 1,3-propane sultone molecules. Finally, the anion exchange with strong acids, HSO_3CF_3, was done by adding 5 g of

HSO_3CF_3 to 5 g of animated pre-dispersed 1,2-dichloroethane at 80 °C for 24 h, and the sample was donated as SO_3-Pr-NH_3-Pr-SBA-15.

2.6. Preparation of stearic acid modified NH_2-Pr-SBA-15 (St- NH_2-Pr-SBA-15)

NH_2-Pr-SBA-15 silica surface modification was performed by adding stearic acid (5 g) to NH_2-Pr-SBA-15 (1g) at a temperature of 140 °C in xylene for 24 hours. After cooling, the precipitate was separated and washed with toluene and then 1,2-dichloroethane to remove the residual stearic acid.

2.7. Preparation of water in oil emulsion (W/O)

A series of emulsions (water in oil) was prepared using mechanical mixing at a speed of 15000 rpm, and the ratio of water (W) to crude oil (O) was varied from 70:30 to 30:70 (W:O) in the presence of 1000 ppm 1-(2-hydroxyethoxy)-nonadecan-2-one. In brief, a definite volume of crude oil (100 ml) was charged in a glass beaker equipped with a magnetic stirrer set at 1000 rpm, at room temperature. A syringe pump added the prescribed amount of water at a rate of 10 mL/h. After reaching the required volume, the stirring was continued at room temperature for a quarter of an hour to ensure homogeneity. The water in oil emulsion is stabilized by 500 ppm St- NH_2-Pr-SBA-15.

2.8. Preparation of oil in water emulsion (O/W)

The preparation of water-in-oil emulsion (W/O) was carried out by dissolving the 0.5% mixture of 1 mole of 1-(2-hydroxyethoxy)-nonadecan-2-one and 0.25 mole of sodium dodecyl sulfate (SDS) in the amount of water. About 100 ppm of active ingredients were withdrawn and diluted the proportion determined for the emulsion preparation. Next, the required amount of crude oil was added to the surfactant solution using the syringe pump at a rate of 1 mL/h. Stirring continued for another quarter of an hour. To stabilize the emulsion, about 500 ppm of the (3-aminopropyl)- triethoxysilane functionalized mesoporous silica, NH_2-Pr-SBA-15, was added, and the solution was stirred for one hour.

3. Results and discussion

3.1 Characterization of the prepared material

The FTIR spectra for SBA-15, NH_2-Pr-SBA-15**,** and SO_3-Pr-NH_3-Pr-SBA-15 were recorded, as shown in **Figure 1a**. As shown in **Figure 1a**, the wideband in the region of 3650 - 3100 cm^{-1} is attributed to the hydroxyl groups of the defective sites as well as the water absorbed on the surface of silica [12]. The strong band at 1093 cm^{-1} corresponds to Si–O framework, and the stretching vibration at 812 cm^{-1} is for the oxygen bridge of silicon-oxygen–silicon [13, 14]. The high energy band at 470 cm^{-1} is due to the bending mode of the silicon framework [11]. After grafting of propylamine, the band at 3650-3100 cm^{-1} became broader due to the superimposing of the –NH group band (stretching mode) with the stretching band of the hydroxyl group of the SBA-15 framework [15]. Additionally, the weak bands at 1578 cm^{-1} and 1632 cm^{-1} are attributed to –NH moieties' bending mode [16]. The bands corresponding to the stretching –CH aliphatic moieties have appeared at 2950 cm^{-1} and 2830 cm^{-1} [17, 18].

Upon protonation, the $–NH_2$ end-capped SBA-15 framework with 1,3-propane sultone molecules after anion exchange with HSO_3CF_3, the strong band at 1093 cm^{-1} of SBA-15 split due to the overlapping of stretching band of sulfur oxygen with SBA-15 band [19]. The shoulder at 1170 cm^{-1} is due to an asymmetric stretching band of SO moieties, while the band at 1387 cm^{-1} is due to the asymmetric stretching mode of the S=O group, which consider as the fingerprint of the sulfonic acid group [20]. Also, the weak deformation band 1471 cm^{-1} is attributed to the formation of $–NH_3$ moieties [21]. The band at 1431 is associated with the carbon-fluoride bond, which further indicates the incorporation of CF_3SO_3 moieties [22, 23]. The FTIR of St- NH_2-Pr-SBA-15 showed an additional band at 1554 cm^{-1}, suggesting the formation of an amide group between the pendant NH_2 and -COOH of stearic acid (**Figure 1b**)

Figure 1c shows the Nitrogen adsorption-desorption isotherm of SBA-15, NH_2-Pr-SBA-15, and SO_3-Pr-NH_3-Pr-SBA-15 materials. The figure shows that the prepared samples exhibited the fourth type (IV) curves, and the capillary condensation step varies between them, as sample SBA-15 appears at 4-6 P/P_0 and decreases with the incorporation of aminosilane and after the exchange by HSO_3CF_3, indicating the success of the introduction of the silane materials and formation of a quaternary ammonium salt [24]. It also shows the desorption hysteresis loop of Type I, which indicates that the pores have formed as a result of accurate silica grouping [25]. The surface area calculated using Brunauer–Emmett–Teller (BET) was 769, 557, and 185 m^2/g for SBA-15, NH_2-Pr-SBA-15 SO_3-Pr-NH_3-Pr-SBA-15 materials, respectively. The pore size of parent silica (SBA-15) was 7.3 nm that deceased upon functionalization with (3-aminopropyl)triethoxysilane, and the reduction in the surface area continued with the addition of 1,3-propane sultone, confirming the attainment of these groups to the solid material (SBA-15) [26].

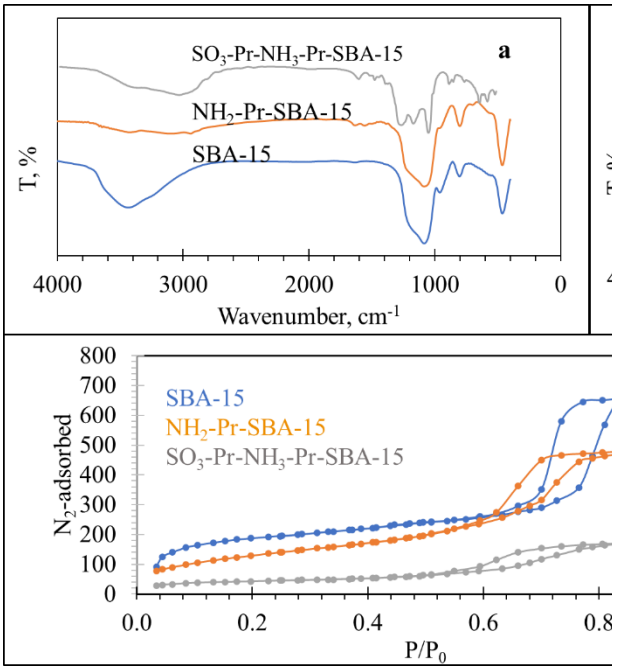

Figure 1. (a-b) FTIR spectra and (c-d) Nitrogen adsorption-desorption isotherm of SBA-15, NH_2-Pr-SBA-15, SO_3-Pr-NH_3-Pr-SBA-15, and St- NH_2-Pr-SBA-15 materials.

Figure 2a-c shows the images obtained by transmission electron microscopy (HRTEM) of SBA-15, NH_2-Pr-SBA-15, SO_3-Pr-NH_3-Pr-SBA-15 materials. The photos show the presence of large pores with a diameter of 4 to 7.5 nm, and their order is well-matched with the recorded crystal directions, (100), (110), and (200) planes (*P6mm* hexagonal symmetry) [27]. The photo also shows that the addition of organosilane groups resulted in a reduction in the pore radius of the material, and this decrease continued with the addition of 1,3-propane sultone and HSO_3CF_3 acid. It is also clear that the material structure was not affected much by branches of an organosilane or after quaternization, but it seemed less orderly. **Figure 2d** shows the XRD of the extracted silica. XRD spectra of silica obtained from rice husk showed broader peaks centered at 2θ-angle of (22.875°), confirming the amorphous nature of the silica. The initial analysis of XRD spectra using Scherrer's formula reveals that the extracted silica has crystallite size in the range of nanoscale. In addition, the SBA-15, NH_2-Pr-SBA-15, and SO_3-Pr-NH_3-Pr-SBA-15 materials showed the only hump centered at ~22°, indicating the mesoporous silicate has a stable silica framework even after functionalization with different materials (**Figure 2e**) [12].

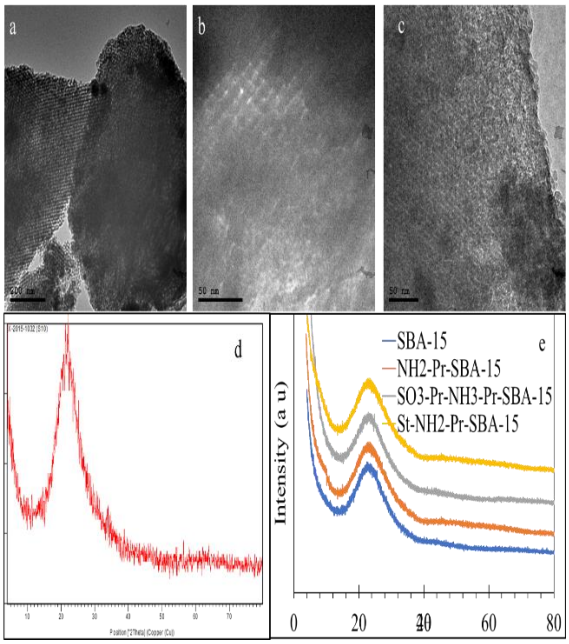

Figure 2. (a-c) transmission electron microscopy (HRTEM) and (c-d) the high angle XRD of extracted silica, SBA-15, NH_2-Pr-SBA-15, SO_3-Pr-NH_3-Pr-SBA-15 materials

3.2 Activity of the catalyst (SO_3-Pr-NH_3-Pr-SBA-15)

The formation of the 1-(2-hydroxyethoxy) nonadecan-2-one was made by esterification of ethylene glycol and stearic acid using the catalyst at x% of the prepared catalyst (SO_3-Pr-NH_3-Pr-SBA-15) by charging 20 g (70.3 mmol) of stearic acid and 4.363549 g (70.30272 moles) ethylene glycol in a round flask equipped with a condenser supplied to the Dean-Stark apparatus. After heating the mixture at 140 ° C, 0.25 g of SO_3-Pr-NH_3-Pr-SBA-15 is added, and the solution is diluted with dry xylene. The collected water was monitored to follow up on the kinetics of the reaction. In addition, the stearic acid transformation rate was found out by withdrawing 0.5 ml from the reaction medium at an equal interval and measuring it with 0.05 N alcoholic potassium hydroxide according to Eq. 1 in the presence of indicator (phenolphthalein).

$$Conversion,\% = \frac{S_i - S_f}{S_i} \times 100 \quad (1)$$

The reaction of stearic acid with ethylene glycol is very difficult and requires a highly acidic catalyst. Experiment with toluene sulfonate catalyst, the results were not more than 26%, at equal molar concentrations, 10% weight, and at a temperature of 140 °C for 36 hours. **Figure 3a** illustrates the relationship between the conversion of stearic acid to the corresponding ester and the time taken to complete

the reaction at conditions estimated at 140 °C, the molar ratio of 1: 1, and different amounts of SO_3-Pr-NH_3-Pr-SBA-15. The catalyst showed a clear efficiency to complete the reaction, and it was found that the percentage of ester formation directly depends on the percentage of the catalyst used. For example, 1% achieved a maximum conversion rate of 52.2% after 26 hours. Increasing the amount of SO_3-Pr-NH_3-Pr-SBA-15 catalyst improved the conversion ratio to nearly 100% (using 8% catalyst). The catalyst's excellent activity is mainly attributed to its distinct structural properties of SO3-Pr-NH3-Pr-SBA-15 catalyst, as SBA-15 material has a cylindrical open-pore and large surface areas. And the presence of the propyl-amine group led to the change of the net charges on the catalyst surface to become hydrophobic, allowing good dispersion in the reaction medium. This hydrophobicity enables good diffusion and gives a greater opportunity for the reactant to entrance the pore of the catalyst, in addition to the good acidity of the catalyst. The FTIR of 1-(2-hydroxyethoxy)-nonadecan-2-one surfactant is shown in **Figure 3b**. The peak at 3356 cm^{-1} is assigned to O-H stretching, the peaks at 2899 and 2836 cm^{-1} correspond to C-H stretching of alkane, the peaks at 1736 cm^{-1} is a characteristic for C=O stretching esters, and the peak at 1,109.83 cm^{-1} is assigned to (C–O–C).

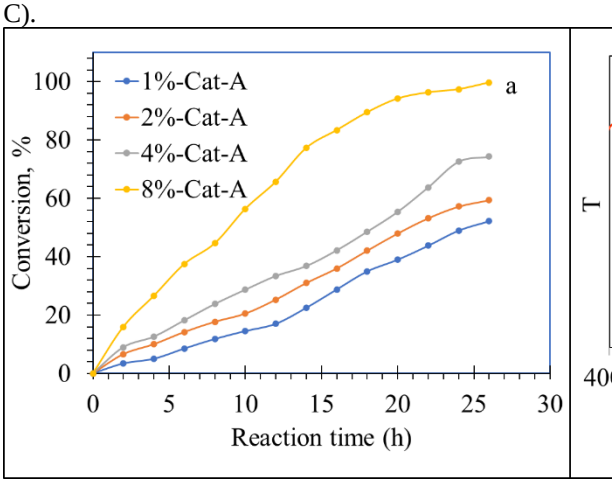

Figure 3. (a) relationship between the amount of the catalyst and conversion; (b) FTIR of 1-(2-hydroxyethoxy) nonadecan-2-one compound

3.2 Study of water in oil emulsion

The composition of crude oil is 12.2 (API gravity at 60 °F), 0.9281 (specific gravity at 60/6 °F), 1.98 (wax content, wt. %), 13.56 (asphaltene content, wt.%) and 15 (pour point, °C). It is clear that the asphaltene content is 13.5%. Asphaltenes are condensed polyaromatic material in the form of sheets; these sheets are interconnected by oxygen (ether), sulfide (S–S), naphthenic ring bonds [28, 29]. The edges of the sheets are end-capped by aliphatic alkyl chains. On the other hand, the structure of resin is to mimic surface-active compounds in which one end that end-capped by alkyl chain is lipophilic, and the other is hydrophilic. In the nonpolar crude oil system, the resin compound's hydrophilic group (polar group) is linked to the asphaltene core, while the nonpolar resin group is linked to the crude oil. The polar asphaltene core is connected to another asphaltene polar core, forming asphaltene aggerates surrounded by resin molecules. These colloidal aggregates are interfacially active when asphaltene is water solvated through hydrogen-bonding interactions with the water. Consequently, a heavy emulsion is formed as a result of the asphaltenes interfacial network [28, 30].

Figure 4 shows the rheological properties of oil-in-water emulsions studied in the presence of 1000 ppm 1-(2-hydroxyethoxy)-nonadecan-2-one and 500 ppm of stearic acid-modified NH_2-Pr-SBA-15 substance. Water-in-oil emulsions contain varying amounts of water, ranging between 30-70%. It is clear that the viscosity increases with increasing the water content of the emulsion due to the increase in the drops number of the water in the prepared emulsions. This increase leads to a rise in the number of hydrogen bonds between water and asphaltene, thus increasing the hydrodynamic radius due to the interaction between water droplets. Consequently, the viscosity of the formed phase is increased. It also shows that the emulsion exhibits remarkable elastic behavior (non-Newtonian) due to the interfacial energy associated with the deformation of the aqueous film formed by water, which leads to increased viscosity [31].

Moreover, previous studies have shown that asphaltene species are likely to form mechanically rigid or viscoelastic interfacial films around water droplets, contributing to more water stability in oil emulsion [32]. Also, the higher viscosity of emulsions proven by hydrophobic molecules is due to the fact that hydrophobic stearic acid-modified aminated silica particles are more attracted to each other in the crude oil phase than of the aqueous phase [33]. The water saturation limit of the crude oil occurs at 70% of the water content. The increase in more water percent during the emulsion preparation results in the emergence of a free water phase in the lower part of the beaker. The amount of water saturation may be to a low ratio of wax content that leads to increasing the tendency to coalesce due to partially increasing the water droplets movement of drops inside the emulsion [34]. Visintin et al. [34] demonstrate that the presence of water above the threshold value can significantly enhance gel formation, changing both the emulsion pour point and the yield strength. Wax molecules can be absorbed into the liquid-liquid interface, increasing the viscosity of the interlayer and reducing the fusion of the droplets forming an emulsion. The viscosity of the differently prepared emulsion is varied with shear

rate, indicating that different dehydrated degrees of the crude oil and all prepared emulsions behave as non-Newtonian fluids. Moreover, all emulsions showed shear thinning behavior (different viscosity values with shear rate).

It is clear that from **Table 1** that the yield stress is decreased with increasing water content in the emulsion, and the results fitted well Casson and Herschel–Bulkley models. The improved flow of the emulsified oil-in-water emulsion may be attributed to preventing the oil droplets from being trapped in the oil, which leads to coalescence through the formation of crystals near the oil interface in the continuous phase (water). The mixed surfactant tends to form small droplets so that it limits droplet aggregation or formation into large droplets or separates from the crude oil as a bulk phase. Yield stress (τ_0) is the minimum stress under which a solid specimen is subjected to permanent deformation or plastic flow without the need for an increase in the applied force or the application of an external force. At the lowest stress, elastic deformation occurs, which disappears with the disappearance of the stress on it, so there is a linear relationship between the elastic deformation and the stress applied to the sample. Above the yield stress, the applied force or stress causes very large deformation of the sample, allowing its flow to begin [1, 35]. The relationship of shear stress and shear rate shows that the yield point decreases for oil-in-water emulsions and is directly proportional to the increase in the amount of water in the emulsion. The yield stress decreases by increasing the amount of water in the emulsion. This means that oil-in-water emulsion needs less energy in a shift than crude oil or water-in-oil emulsions.

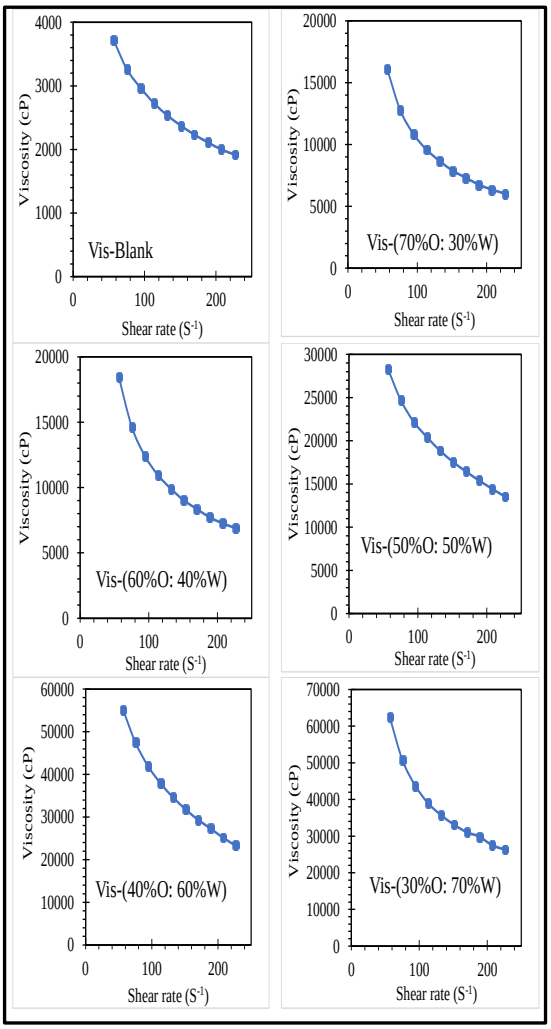

Figure 4. effect of water fraction on viscosity for W/O emulsion

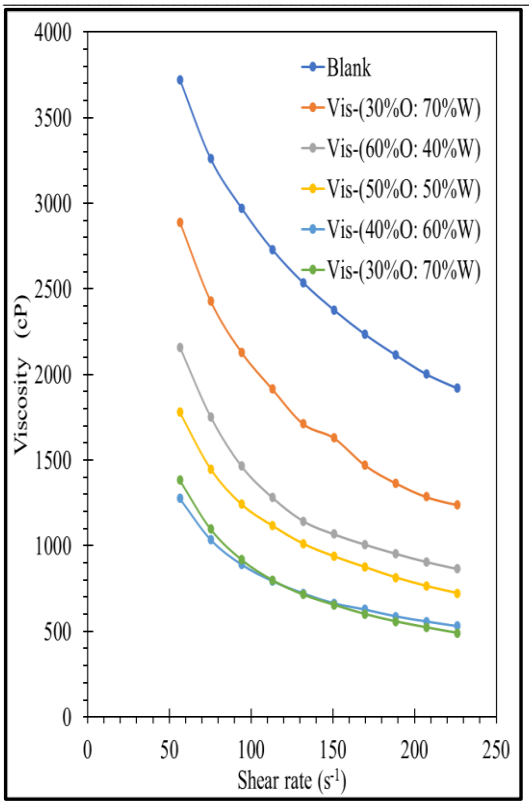

Figure 5. The viscosity of oil in water emulsion at different oil content ratios

3.2.1. Rheological models

By studying the results of water-in-oil emulsions at different water ratios from 30-70% concerning Power's law (**Eq. 2**; the parameters K and n are consistency index and flow index), it was found that the emulsions show the pseudoplastic behavior, and the flow index "n" was within the range of 0.29 to 0.38 (**Table 1**). It has been reported that if n>1 (the fluid showed dilatant behavior); if n<1 (the fluid showed pseudoplastic behavior), and if n=1 (the fluid showed Newtonian behavior) [36, 37]. The flow index "n" increases with increasing water in the emulsion tell 50% water and become decease again, reaching 0.3842 for 70% water. The pseudoplastic behavior (Newtonian fluid) trend results from separating the emulsion components from each other due to the collapse of the three-dimensional network water droplets; however, the ratio of 70% water may be divided easier. From the Bingham model (**Eq. 3**), it is clear that the τ_0 (yield stress) is increased from 1635.6 D/cm^3 to 7735.8 D/cm^3, 8843.0 D/cm^3, 12562 D/cm^3, 27077 D/cm^3, and 27788 D/cm^3, as water content increases from 30% to 70% due to continued dispersion of oil droplets in the oil phase. Also, the plastic viscosity is increased because of the formation of the network structure.

$$\tau = KD^n \quad \text{Eq. 2}$$

$$\log(\tau) = \log(k) + n\log(D)$$

$$\tau(\text{shear stress}) = \tau_0(\text{Yield Stress}) + \eta(\text{Plastic Viscosity}) \times D(\text{shear rate}) \quad \text{(Eq.3)}$$

The Casson model describes a non-Newtonian fluid with yield stress and can be expressed as **Eq. 4.**

$$\sqrt{\tau} = \sqrt{\tau_0} + \sqrt{\eta D} \quad \text{Eq.4}$$

Where the symbols τ, τ_0, η and D are shear rate, yield stress, plastic viscosity, and shear stress, respectively. The yield stress obtained from the Casson model multiplied many times after water formation in oil emulsion. The τ_0 of crude oil was 725.1 D/cm^{3,} which reaches 16702.98 D/cm^3 for emulsion containing 70% water. Along the same lines, the results of plastic viscosity appear. The Herschel-Bulkley is used to predict non-Newtonian fluid behavior (**Eq. 5**).

$$\tau = \tau_0 + KD^n \quad \text{Eq. 5}$$

$$\log(\tau - \tau_0) = \log(\mathrm{K}) + n\log(D)$$

The n values were 0.9736, 1.0525, 1.0583, 1.1534, 1.2395, and 1.0063 for crude oil and 30-70% water content, respectively, while the K values were 14.9589 D/cm^3 for crude oil and increased by increasing the amount of water in the emulsion up to 70%. The results fit the Herschel-Bulkley model and Casson model.

By the preparing emulsion in the presence of 0.5% mixture of 1 mole of 1-(2-hydroxyethoxy)-nonadecan-2-one, 0.25 mole of sodium dodecyl sulfate (SDS) and 500 ppm of NH_2-Pr-SBA-15 (CMS of sodium dodecyl sulfate and 1-(2-hydroxyethoxy)-nonadecan-2-one are 7.8x10^{-4} M; and 4.5 x10^{-5} M at 25 °C). **Figure 5** shows the relationship between shear rate (s^{-1}) and oil viscosity of the crude oil-water emulsion. It is clear that the viscosity of all prepared emulsions is lower than the crude oil, where the viscosity is decreased by decreasing the oil ratio in the emulsion. The emulsion showed stability of up to 18 hours. The addition of the surfactant mixture with amine-terminated silica to the emulsion made the system stable due to the tendency of asphaltene particles to adsorb at the oil-water interface. The ionic nature of SDS increases the ionization of the system and increases the solubility of nonionic surfactants (-(2-hydroxyethoxy)-nonadecan-2-one) that dissolve in the system through hydrogen bonding.

Table 1. Rheological models of W/O and O/W emulsion stabilized with modified silica

	Water in oil emulsion			**Oil in water emulsion**		
Bingham model	τ_0(D/cm^3)	η_p (cP)	R^2	τ_0(D/cm^3)	η_p (cP)	R^2
Blank	1635.6	12.368	0.9804			
70%O: 30%W	7735.8	26.766	0.9727	907.46	3.8313	0.9893
60%O: 40%W	8843.0	30.599	0.9728	761.28	3.7908	0.9776
50%O: 50%W	12562	86.335	0.9667	700.51	3.1967	0.9729
40%O: 60%W	27077	126.49	0.9375	514.95	2.8363	0.9887
30%O: 70%W	27788	144.41	0.9542	395.63	2.5881	0.9709
Casson model	τ_0 (D/cm3)	ηp (cP)	R^2	τ_0 (D/cm3)	ηp (cP)	R^2
Blank	725.1172	28.959	0.995			
70%O: 30%W	5408.573	65.779	0.9984	605.16	1.31	0.9929
60%O: 40%W	6196.366	78.618	0.9985	473.15	1.55	0.9992
50%O: 50%W	6497.65	80.608	0.9840	452.115	1.167	0.9907
40%O: 60%W	16458.32	128.29	0.9640	312.122	1.14896	0.9822
30%O: 70%W	16702.98	130.4	0.9957	227.165	1.133	0.9661
Power model	k	n	R^2	k	n	R^2
Blank		0.5016	0.9682			
70%O: 30%W	258.702	0.2982	0.9739	286.68	0.3308	0.9775
60%O: 40%W	2677.32	0.2984	0.9844	206.3	0.3752	0.9631
50%O: 50%W	6723.57	0.4775	0.9639	179.97	0.3815	0.9602
40%O: 60%W	2376.84	0.3877	0.974	135.519	0.3897	0.964
30%O: 70%W	7118.69	0.3842	0.9882	96.3163	0.4213	0.939
Herschel–Bulkley model	n	R^2	k	n	R^2	k
Blank	0.9736	0.9912	14.9589			
70%O: 30%W	1.0525	0.9934	16.4778	0.621225	0.9969	11.4815
60%O: 40%W	1.0583	0.993	22.8139	0.7266	0.9972	4.45862
50%O: 50%W	1.1534	0.9596	40.0682	0.737025	0.99	3.48899
40%O: 60%W	1.2395	0.9209	38.0365	0.73245	0.983	3.18127
30%O: 70%W	1.0063	0.9972	141.579	0.707325	0.9872	3.42295

Conclusion

Silica was extracted from ricehusk, treated with sodium hydroxide, and added to an aqueous solution containing a Pluronic surfactant (P123) to turn the extracted silica into mesoporous silicate (SBA-15). The microscopic analysis confirmed the formation of mesoporous silica with tunable pores and a considerable surface area, approaching 700 m^2/g. The SBA-15 surface was grafted with (3-aminopropyl)triethoxysilane, and some chemical reactions were performed to produce an SBA-15 end-capped with a highly acidic group, – SO_3CF_3. The catalyst has achieved results up to 99.9% in the esterification of ethylene glycol with stearic acid. The resultant ester, 1-(2-hydroxyethoxy)-nonadecan-2-one, was mixed with sodium dodecyl sulfate to make oil in water emulsion stabilized with aminosilane nanoparticle. The emulsion showed stability for about

18 hours and also showed a high reduction in viscosity. Some rheological models, such as Power, Herschel–Bulkley, Casson, and Bingham models, were used to analyze the oil in water and water in oil emulsions. The emulsion filled well Casson and Herschel–Bulkley models.

References

[1] S.W. Hasan, M.T. Ghannam, N. Esmail, Heavy crude oil viscosity reduction and rheology for pipeline transportation, Fuel 89(5) (2010) 1095-1100.
[2] M.A. Kessick, C.E.S. Denis, Pipeline transportation of heavy crude oil, Google Patents, 1982.
[3] S. Kumar, V. Mahto, Emulsification of Indian heavy crude oil in water for its efficient transportation through offshore pipelines, Chemical Engineering Research and Design 115 (2016) 34-43.
[4] W. Loh, R.S. Mohamed, R.G. dos Santos, Crude oil asphaltenes: colloidal aspects, Encyclopedia of surface and colloid science, CRC Press2015, pp. 1546-1562.
[5] J. Lim, S. Wong, M. Law, Y. Samyudia, S. Dol, A review on the effects of emulsions on flow behaviours and common factors affecting the stability of emulsions, JApSc 15(2) (2015) 167-172.
[6] N. Garti, Progress in stabilization and transport phenomena of double emulsions in food applications, LWT-Food Science and Technology 30(3) (1997) 222-235.
[7] H. Okochi, M. Nakano, Preparation and evaluation of w/o/w type emulsions containing vancomycin, Advanced drug delivery reviews 45(1) (2000) 5-26.
[8] J.S. Lee, J.W. Kim, S.H. Han, I.S. Chang, H.H. Kang, O.S. Lee, S.G. Oh, K.D. Suh, The stabilization of L-ascorbic acid in aqueous solution and water-in-oil-in-water double emulsion by controlling pH and electrolyte concentration, International Journal of Cosmetic Science 26(4) (2004) 217-217.
[9] A. Bensakhria, Y. Peysson, G. Antonini, Experimental study of the pipeline lubrication for heavy oil transport, Oil & gas science and technology 59(5) (2004) 523-533.
[10] A. Hart, A review of technologies for transporting heavy crude oil and bitumen via pipelines, Journal of Petroleum Exploration and Production Technology 4(3) (2014) 327-336.
[11] M.A. Betiha, Y.M. Moustafa, M.F. El-Shahat, E. Rafik, Polyvinylpyrrolidone-Aminopropyl-SBA-15 schiff Base hybrid for efficient removal of divalent heavy metal cations from wastewater, Journal of Hazardous Materials 397 (2020) 122675.
[12] H.M.A. Hassan, M.A. Betiha, R.F.M. Elshaarawy, M. Samy El-Shall, Promotion effect of palladium on Co3O4 incorporated within mesoporous MCM-41 silica for CO Oxidation, Applied Surface Science 402 (2017) 99-107.
[13] M.A. Betiha, Y.M. Moustafa, A.S. Mansour, E. Rafik, M.F. El-Shahat, Nontoxic polyvinylpyrrolidone-propylmethacrylate-silica nanocomposite for efficient adsorption of lead, copper, and nickel cations from contaminated wastewater, Journal of Molecular Liquids 314 (2020) 113656.
[14] M.A. Betiha, G.G. Mohamed, N.A. Negm, M.F. Hussein, H.E. Ahmed, Fabrication of ionic liquid-cellulose-silica hydrogels with appropriate thermal stability and good salt tolerance as potential drilling fluid, Arabian Journal of Chemistry 13(7) (2020) 6201-6220.
[15] Z.A. Alrowaili, I.H. Alsohaimi, M.A. Betiha, A.A. Essawy, A.A. Mousa, S.F. Alruwaili, H.M.A. Hassan, Green fabrication of silver imprinted titania / silica nanospheres as robust visible light-induced photocatalytic wastewater purification, Materials Chemistry and Physics 241 (2020) 122403.
[16] M.A. Betiha, S.B. El-Henawy, A.M. Al-Sabagh, N.A. Negm, T. Mahmoud, Experimental evaluation of cationic-Schiff base surfactants based on 5-chloromethyl salicylaldehyde for improving crude oil recovery and bactericide, Journal of Molecular Liquids 316 (2020) 113862.
[17] A.M. Rabie, H.M. Abd El-Salam, M.A. Betiha, H.H. El-Maghrabi, D. Aman, Mercury removal from aqueous solution via functionalized mesoporous silica nanoparticles with the amine compound, Egyptian Journal of Petroleum 28(3) (2019) 289-296.
[18] M.A. Betiha, A.M. Rabie, A.M. Elfadly, F.Z. Yehia, Microwave assisted synthesis of a VOx-modified disordered mesoporous silica for ethylbenzene dehydrogenation in presence of CO2, Microporous and Mesoporous Materials 222 (2016) 44-54.
[19] N.A. Negm, M.A. Betiha, M.S. Alhumaimess, H.M.A. Hassan, A.M. Rabie, Clean transesterification process for biodiesel production using heterogeneous polymer-heteropoly acid nanocatalyst, Journal of Cleaner Production 238 (2019) 117854.
[20] L. Wang, J. Zhang, S. Yang, Q. Sun, L. Zhu, Q. Wu, H. Zhang, X. Meng, F.-S. Xiao, Sulfonated hollow sphere carbon as an efficient catalyst for acetalisation of glycerol, Journal of Materials Chemistry A 1(33) (2013) 9422-9426.
[21] M.A. Betiha, M.F. Menoufy, A.M. Al-Sabagh, H.M.A. Hassan, S.A. Mahmoud, Acidic mesostructured aluminosilicates assembled from economic acidic template characterized by catalytic cracking reactions, Microporous and Mesoporous Materials 204 (2015) 15-24.
[22] J. Scaranto, A.P. Charmet, S. Giorgianni, IR spectroscopy and quantum-mechanical studies of the adsorption of CH2CClF on TiO2, The Journal of Physical Chemistry C 112(25) (2008) 9443-9447.
[23] F. Liu, S. Zuo, W. Kong, C. Qi, High-temperature synthesis of strong acidic ionic liquids functionalized,

ordered and stable mesoporous polymers with excellent catalytic activities, Green Chemistry 14(5) (2012) 1342-1349.
[24] H.M.A. Hassan, M.A. Betiha, S.K. Mohamed, E.A. El-Sharkawy, E.A. Ahmed, Salen- Zr(IV) complex grafted into amine-tagged MIL-101(Cr) as a robust multifunctional catalyst for biodiesel production and organic transformation reactions, Applied Surface Science 412 (2017) 394-404.
[25] H.M.A. Hassan, E.M. Saad, M.S. Soltan, M.A. Betiha, I.S. Butler, S.I. Mostafa, A palladium(II) 4-hydroxysalicylidene Schiff-base complex anchored on functionalized MCM-41: An efficient heterogeneous catalyst for the epoxidation of olefins, Applied Catalysis A: General 488 (2014) 148-159.
[26] Z.M.H. Kheiralla, A.A. Rushdy, M.A. Betiha, N.A.N. Yakob, High-performance antibacterial of montmorillonite decorated with silver nanoparticles using microwave-assisted method, Journal of Nanoparticle Research 16(8) (2014) 2560.
[27] S.K. Mohamed, A.A. Ibrahim, A.A. Mousa, M.A. Betiha, E.A. El-Sharkawy, H.M.A. Hassan, Facile fabrication of ordered mesoporous Bi/Ti-MCM-41 nanocomposites for visible light-driven photocatalytic degradation of methylene blue and CO oxidation, Separation and Purification Technology 195 (2018) 174-183.
[28] A.P. Sullivan, P.K. Kilpatrick, The Effects of Inorganic Solid Particles on Water and Crude Oil Emulsion Stability, Industrial & Engineering Chemistry Research 41(14) (2002) 3389-3404.
[29] T.F. Yen, The colloidal aspect of a macrostructure of petroleum asphalt, Fuel science & technology international 10(4-6) (1992) 723-733.
[30] C. Bardon, L. Barre, D. Espinat, V. Guille, M.H. Li, J. Lambard, J. Ravey, E. Rosenberg, T. Zemb, The colloidal structure of crude oils and suspensions of asphaltenes and resins, Fuel science and technology international 14(1-2) (1996) 203-242.
[31] T.S.T. Ariffin, E. Yahya, H. Husin, The Rheology of Light Crude Oil and Water-In-Oil-Emulsion, Procedia Engineering 148 (2016) 1149-1155.
[32] M.C.K. de Oliveira, L.R. Miranda, A.B. de Carvalho, D.F.S. Miranda, Viscosity of Water-in-Oil Emulsions from Different American Petroleum Institute Gravity Brazilian Crude Oils, Energy & Fuels 32(3) (2018) 2749-2759.
[33] P.K. Kilpatrick, Water-in-crude oil emulsion stabilization: review and unanswered questions, Energy & Fuels 26(7) (2012) 4017-4026.
[34] R.F.G. Visintin, T.P. Lockhart, R. Lapasin, P. D'Antona, Structure of waxy crude oil emulsion gels, Journal of Non-Newtonian Fluid Mechanics 149(1) (2008) 34-39.
[35] M.T. Ghannam, N. Esmail, Yield stress behavior for crude oil–polymer emulsions, Journal of Petroleum Science and Engineering 47(3) (2005) 105-115.
[36] G. Schramm, A practical approach to rheology and rheometry, Haake Karlsruhe1994.
[37] T. Mezger, The rheology handbook, Vincentz Network2020.